Evaluating the Influence of Plant-Specific Physiological Parameterizations on the Partitioning of Land Surface Energy Fluxes

MAURO SULIS,* MATTHIAS LANGENSIEPEN,+ PRABHAKAR SHRESTHA,* ANKE SCHICKLING,# CLEMENS SIMMER,@ AND STEFAN J. KOLLET&

* *Meteorological Institute, University of Bonn, Bonn, Germany*
+ *Institute of Crop Science and Resource Conservation, University of Bonn, Bonn, Germany*
# *Institute for Bio- and Geosciences, Plant Sciences (IBG-2), Forschungszentrum Jülich, Jülich, Germany*
@ *Meteorological Institute, University of Bonn, Bonn, and Centre for High-Performance Scientific Computing in Terrestrial Systems, Geoverbund ABC/J, Jülich, Germany*
& *Institute for Bio- and Geosciences, Agrosphere (IBG-3), Forschungszentrum Jülich, and Centre for High-Performance Scientific Computing in Terrestrial Systems, Geoverbund ABC/J, Jülich, Germany*

(Manuscript received 14 August 2014, in final form 13 November 2014)

ABSTRACT

Plant physiological properties have a significant influence on the partitioning of radiative forcing, the spatial and temporal variability of soil water and soil temperature dynamics, and the rate of carbon fixation. Because of the direct impact on latent heat fluxes, these properties may also influence weather-generating processes, such as the evolution of the atmospheric boundary layer (ABL). In this work, crop-specific physiological characteristics, retrieved from detailed field measurements, are included in the biophysical parameterization of the Terrestrial Systems Modeling Platform (TerrSysMP). The physiological parameters for two typical European midlatitudinal crops (sugar beet and winter wheat) are validated using eddy covariance fluxes over multiple years from three measurement sites located in the North Rhine–Westphalia region of Germany. Comparison with observations and a simulation utilizing the generic crop type shows clear improvements when using the crop-specific physiological characteristics of the plant. In particular, the increase of latent heat fluxes in conjunction with decreased sensible heat fluxes as simulated by the two crops leads to an improved quantification of the diurnal energy partitioning. An independent analysis carried out using estimates of gross primary production reveals that the better agreement between observed and simulated latent heat adopting the plant-specific physiological properties largely stems from an improved simulation of the photosynthesis process. Finally, to evaluate the effects of the crop-specific parameterizations on the ABL dynamics, a series of semi-idealized land–atmosphere coupled simulations is performed by hypothesizing three cropland configurations. These numerical experiments reveal different heat and moisture budgets of the ABL using the crop-specific physiological properties, which clearly impacts the evolution of the boundary layer.

1. Introduction

Vegetation constitutes a major component of the interface between the land surface and atmosphere compartments of the terrestrial water, energy, and matter cycle. As a dominant land cover, it exerts a major impact on both climate (Betts et al. 1997; Douville et al. 2000) and weather dynamics (Pielke 2001; Garcia-Carreras et al. 2010) by modifying the radiation, momentum, water, CO_2, and energy balance of and the fluxes between the land surface and the atmospheric boundary layer (ABL; Arora 2002). Land-cover change alters albedo, surface runoff, roughness height, and as a consequence the land surface energy partitioning (Kueppers et al. 2007; Georgescu et al. 2009; Davin and de Noblet-Ducoudré 2010). The large-scale transformation of native lands into agricultural production (Foley et al. 2005) has increased the interest in exploring the specific role of croplands in the estimation of the energy, water, and carbon budgets ranging from daily (McPherson et al. 2004; Haugland and Crawford 2005) to multiyear time scales (de Noblet-Ducoudré et al. 2004; Bondeau et al. 2007).

Denotes Open Access content.

Corresponding author address: Mauro Sulis, Meteorological Institute, University of Bonn, Meckenheimer Allee 176, 53115 Bonn, Germany.
E-mail: msulis@uni-bonn.de

DOI: 10.1175/JHM-D-14-0153.1

In Earth system modeling platforms, the vegetation is represented as one of several possible biomes (Niu et al. 2011) or, when using subgrid mosaics, as multiple biomes (Oleson et al. 2008). These biomes are defined by vegetation characteristics (e.g., aerodynamic, optical, rooting depth, and photosynthesis properties) of individual species or plant functional types that do have measurable leaf physiology and carbon allocation (Bonan et al. 2002). The physiological parameterizations associated with these plant functional types have been tested at local, regional, and continental scales using point and gridded information of energy and carbon fluxes (Morales et al. 2005; Friend et al. 2007; Stöckli et al. 2008; Mahecha et al. 2010; Bonan et al. 2011), contributing significantly to the identification of land surface model deficiencies (Bonan et al. 2012). However, because of the lack of constraining plant ecophysiological parameterizations with independent measurements, the uncertainty associated with these parameters remains large (Lu et al. 2013).

Several studies have examined the performances of land surface models in simulating energy partitioning, soil water dynamics, and carbon fluxes in field crops. For example, Arora (2003) evaluated the performance of a coupled land surface [Canadian Land Surface Scheme (CLASS)] and ecosystem model against energy (net radiation, latent heat, and sensible heat) and carbon fluxes in a winter wheat field at the Oklahoma (Ponca City) AmeriFlux site. Similarly, Kothavala et al. (2005) compared the results of the CLASS model with eddy covariance flux data measured over four cultivated crop types (maize, soybean, wheat, and millet). Ingwersen et al. (2011) assessed the accuracy of the Noah land surface model with respect to energy flux and soil water content measurements for a winter wheat stand. Van den Hoof et al. (2011) validated the coupled Joint U.K. Land Environment Simulator (JULES) and Simple and Universal Crop Growth Simulator (SUCROS) model, JULES–SUCROS, using energy fluxes (latent and sensible heat) and gross primary production measurements at six Flux Network (FLUXNET) sites over Europe. The value of a detailed description of root growth and water uptake processes in simulating the seasonal patterns of evapotranspiration and soil moisture in a winter wheat field has been investigated by Gayler et al. (2013) using the Community Land Model, version 3.5 (CLM3.5). Five crop models with different degrees of complexity in describing plant processes were compared to CLM3.5 by Wöhling et al. (2013). The ensemble of models was benchmarked against soil moisture dynamics, evapotranspiration, and leaf area index at two winter wheat fields. Finally, Gayler et al. (2014) enhanced the multioption framework of the Noah-MP land surface model by including an agricultural crop submodule that dynamically simulates root growth processes. The performance of the improved model was evaluated at a winter wheat field site using eddy covariance (latent, sensible, and ground heat) and soil moisture measurements.

These studies developed strategies to overcome shortcomings of land surface models in simulating detailed field-scale energy and carbon exchanges by introducing additional processes (e.g., dynamic plant phenology, root growth) and/or by improving model parameterizations (e.g., time-variable minimum stomatal resistance). In doing so, they interpreted land surface scheme performance by lumping the variety of crop physiological parameters into a few generic classes (e.g., Nemani and Running 1996; Kucharik et al. 2000) that were mostly intended for global and regional-scale model applications. There exists, however, a large number of field experimental studies (e.g., Moureaux et al. 2006; Suyker and Verma 2009; Aubinet et al. 2009) that have documented the widely varying responses of different crops in the exchange fluxes between the land and the atmosphere. These responses strongly depend on crop-specific physiological characteristics such as photosynthesis (Baldocchi 1994), effects of carbon and nitrogen metabolisms on stomatal regulation (Schulze et al. 1994), plant hydraulic properties (Buckley 2005), transpiration control (Franks et al. 2007), phenology, and growth (Hay and Porter 2006).

The influence of cropland ecosystems on land–atmosphere interactions and ABL dynamics has been evaluated in a number of modeling studies. Among others, Tsvetsinskaya et al. (2001) found that replacing a generic crop formulation with the more realistic representation of corn from a crop model leads to improvements in the simulated leaf area index over the central Great Plains region of North America. These improvements generate differences in the simulated turbulent heat fluxes, which lead to changes in temperature, humidity, winds, and precipitation. McPherson and Stensrud (2005) evaluated the effect of replacing tallgrass prairie with winter wheat on the evolution of the ABL in the Great Plains (Oklahoma). Here, the increased values of latent heat and atmospheric moisture near the surface resulting from the growing crop ultimately lead to a shallower ABL. Levis et al. (2012) quantified the effect of an explicit representation of planting and harvesting activities in the simulated land surface energy fluxes over the midwestern North America. The resulting modifications in the heat fluxes produce changes in the precipitation that agree better with observations. While these studies provided many useful insights on the effects of common features of cropland ecosystems (e.g., crop-specific phenology, rotation, and management activities) on large regional-scale processes, there have been few studies that assessed the

extent to which a more accurate physiological characterization of diverse crop species could affect the modeling of land–atmosphere interactions.

The objective of this study is to examine the impact of crop-specific physiological parameterizations on the partitioning of the simulated land surface energy fluxes, and to assess the resulting influence on the estimation of the heat and moisture budgets of the ABL. The underlying hypothesis is that the large uncertainty usually associated with generic biome parameterizations could explain land surface model deficiencies in reproducing point measurements of energy and CO_2 fluxes. In this context, a new set of parameters that account for the physiological diversity of two crops—sugar beet and winter wheat—is included in the land surface component (CLM3.5) of the Terrestrial Systems Modeling Platform (TerrSysMP) recently presented by Shrestha et al. (2014). These new parameters are based on comprehensive field measurements of photosynthesis characteristics, gas exchange, nutrient balances, and optical properties of the two plants. The performance of the model with this set of model parameters is evaluated using energy and CO_2 fluxes from eddy covariance measurements conducted during several years at three sites located in North Rhine–Westphalia, Germany. In addition, the impact of this more detailed representation of vegetation characteristics on the modeling of land surface–atmosphere interactions is evaluated by designing a set of coupled numerical experiments. The simulations consist of 48-h semi-idealized hindcast runs over the region, where a generic crop plant functional type is replaced with the region-specific sugar beet and winter wheat parameterizations.

2. Materials and methods

a. Field sites and observations

The three field sites selected in this study (Merken, 50°50′N, 6°23′E; Selhausen, 50°52′N, 6°26′E; and Merzenhausen, 50°55′N, 6°17′E) are located in the western part of Germany near the Belgian border (Fig. 1). The study area is situated in the southern part of the lower Rhine embayment within the Rur catchment. The dominant land-use types are forest, grassland, and cropland, with cereals (e.g., winter wheat) and sugar beet the main cultivated crops. The regional climate can be characterized as temperate maritime with a mean annual temperature of 9.9°C and precipitation of 698 mm (1961–2008, German weather service station Jülich, Stat-ID 2474). The soil is classified as a clay loam (IUSS 2006) with the underlying Quaternary sediments originating mostly from fluvial deposits from the Rhine–Meuse and the Rur river systems.

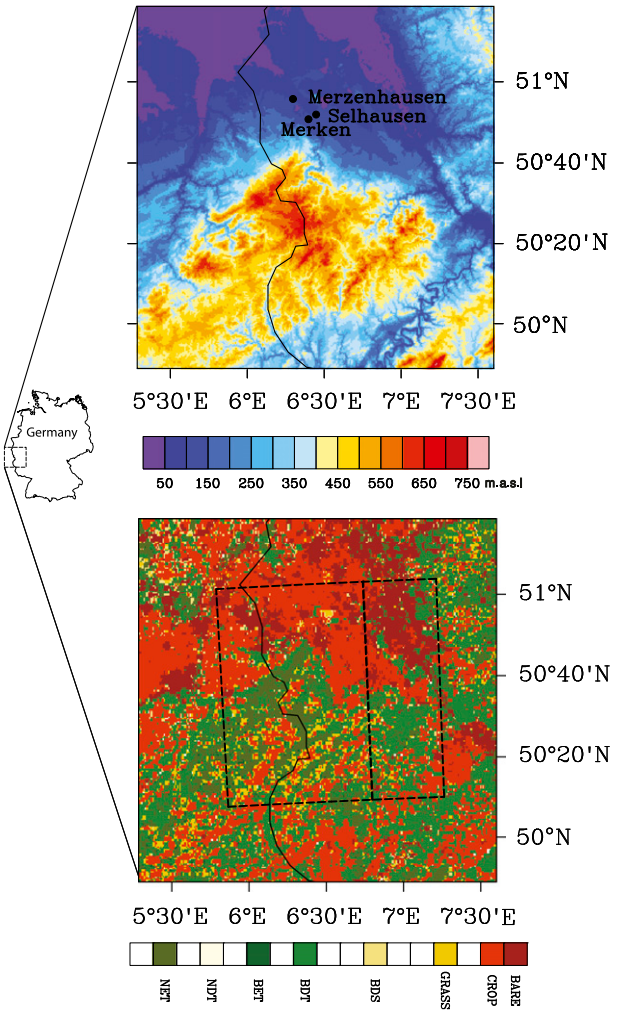

FIG. 1. (top) Topographic and (bottom) land-use map of the study area showing the location of the three measurement sites. For the land-use map, the dominant vegetation classes are needleleaf evergreen tree (NET), needleleaf deciduous tree (NDT), broadleaf evergreen tree (BET), broadleaf deciduous tree (BDT), broadleaf deciduous shrub (BDS), grassland (GRASS), crop (CROP), and barren soil (BARE).

Sugar beet (*Beta vulgaris*; variety Lucata) was grown in Merken (2009) and Selhausen (2011), and winter wheat (*Triticum aestivum*; variety Raspail) was grown in Merzenhausen (2012) and Selhausen (2013). Winter wheat is sown in autumn, vernalizes (i.e., prolonged exposure to low temperatures) during winter, rapidly develops its leaf area during spring, and reaches peak transpiration rates during anthesis (i.e., opening of the flower) in early summer. During this time, the crop is particularly susceptible to water stress; transpiration decreases rapidly, however, with progressing senescence. At the field site, winter wheat is commonly harvested in July. Sugar beet is sown in spring, rapidly develops its full leaf area toward summer, and then maintains the leaf area until harvest in late autumn.

Latent heat, sensible heat, and net ecosystem exchange were continuously monitored with eddy covariance systems. Wind speed and air temperature were measured with an ultrasonic anemometer (CSAT3; Campbell Scientific, Inc., Logan, Utah). Measurements of water vapor and carbon dioxide were carried out using an open-path infrared gas analyzer (LI7500; LI-COR, Inc., Lincoln, Nebraska). Measurements were taken with a sampling rate of 20 Hz and collected as raw time series using a high-performance datalogger (CR5000; Campbell Scientific, Inc.). Fluxes of latent heat, sensible heat, and net ecosystem exchange were estimated from the covariances between the measured 30-min-long high-frequency time series of the vertical wind speed and water vapor content, temperature, and CO_2, respectively, by Reynolds averaging (Reynolds 1894). Additional information (e.g., on quality control, uncertainty assessment, and comparison with other measurement techniques) of the eddy covariance measurements used in this study can be found in Graf et al. (2013) and Mauder et al. (2013).

The net ecosystem exchange (NEE) measurements available at the selected sites were partitioned into gross primary production (GPP) and ecosystem respiration R_{eco}. This flux partitioning was performed using the Lloyd-and-Taylor model (Lloyd and Taylor 1994) to calculate time series of R_{eco} and estimating GPP as a residual:

$$R_{eco}(T_{air}) = R_{eco,ref} e^{E_0[1/(T_{ref}-T_0)-1/(T_{air}-T_0)]} \quad \text{and} \qquad (1)$$

$$\mathrm{GPP} = \mathrm{NEE} - R_{eco}, \qquad (2)$$

where $R_{eco,ref}$ (μmol m^{-2} s^{-1}) is the respiration at reference temperature T_{ref} (K); E_0 (K) is the activation energy; and T_0 (K) and T_{air} (K) are the base and air temperature, respectively. To avoid overparameterization, T_0 was kept constant at 227.13 K (Richardson and Hollinger 2005) and T_{ref} was set to 283.15 K (Lloyd and Taylor 1994). Values of $R_{eco,ref}$ and E_0 were estimated by fitting Eq. (1) over nighttime to R_{eco} versus air temperature using the least squares method.

b. *Plant physiological parameterizations*

The plant physiological parameters of the sugar beet and winter wheat specific crop types are summarized in Table 1. The values of these parameters result from a synthesis of several field measurement campaigns [for an overview, see Schickling et al. (2010)] carried out at several sites located in the agricultural region around Jülich, Germany, between 2008 and 2013. The list of parameters is grouped into three main classes, which characterize the photosynthesis, optical, and aerodynamic properties of the two crop types. The values for the standard generic C_3 crop type parameterization of CLM3.5 are also shown for comparison (ctrl crop). The root distribution parameters were kept unchanged from the control configuration because of the lack of detailed in situ information.

Parameters needed for solving the photosynthesis equations were based on leaf-level photosynthesis measurements carried out with a standard open-path gas-exchange system equipped with blue and red light sources for controlling impinging photosynthetically active radiation (Model LI6400 XT; LI-COR, Inc.). Maximum rates of carboxylation at 25°C $Vcmax_{25}$ for both crops were derived from measured photosynthetic rate responses to automatically controlled CO_2 levels in the leaf cuvette, which was kept at a constant temperature of 25°C. Photosynthetically active radiation was set to 1000 and 1800 μmol m^{-2} s^{-1} during each measurement, which corresponds to light saturation condition for sugar beet and winter wheat, respectively. The value of $Vcmax_{25}$ is internally calculated by the model as described by Thornton and Zimmermann (2007), the values in Table 1 are thus reported for the completeness of the conducted measurements. The slope of conductance-to-photosynthesis relationship mp was determined by regressing measured stomatal conductances against the corresponding measured Ball–Woodrow–Berry indices (Ball et al. 1987). The CO_2 assimilation rates, relative humidity, and CO_2 mole fractions at the leaf surfaces were measured for several daily cycles and averaged over the main growing periods of the sugar beet and winter wheat crops. The quantum efficiency qe_{25} was determined from light response curves established at 25°C leaf surface temperature. Specific leaf areas at the top of the sugar beet and winter wheat canopies sla_{top} were estimated based on information from the literature (Wullschleger 1993). The ratio between specific leaf area and leaf area index d_{SLA}:d_{LAI}, which is used to calculate the specific sunlit and shaded projected leaf area index, was set to zero for sugar beet and winter wheat as in the case for the control crop. Leaf samples for carbon and nitrogen content analysis were taken at biweekly intervals, oven dried at 65°C temperature, ground (Model MM400; Retsch GmbH, Haun, Germany), and then processed with a CN analyzer (Elementaranalysator Euro EA; HEKAtech, Wegburg, Germany). The resulting $leaf_{C:N}$ parameter values were averaged over the main growing periods. Sugar beet and winter wheat fractions of leaf nitrogen in the Rubisco enzyme fl_{N_R} were set to 0.15 (Raab and Norman 1994) and 0.3 (Lawlor 2002), respectively. Values for soil water potentials at stomatal opening $smps_o$ and closure $smps_c$ were estimated referring to Wesseling et al. (1991). The value of $smps_o$ for sugar beet varies between −3200 and −6000 mm, depending on

TABLE 1. Plant physiological parameters. Variables are defined in the text except for the leaf reflectance (visible, near-infrared) $\text{rho}_{\text{vis,nir}}$, stem reflectance (visible, near-infrared) $\text{rho}_{\text{vis,nir}}$, leaf transmittance (visible, near-infrared) $\text{tau}_{\text{vis,nir}}$, and stem transmittance (visible, near-infrared) $\text{tau}_{\text{vis,nir}}$.

	Photosynthetic parameters									Optical properties				Aerodynamic properties		
Crop	Vcmax_{25} [(μmol CO_2) m^{-2} s^{-1}]	mp	qe_{25} [(μmol CO_2) (μmol photon)$^{-1}$]	sla_{top} (m^2 gC^{-1})	$d_{\text{SLA}}:d_{\text{LAI}}$ (m^2 gC)	leaf_{CN} (gC gN^{-1})	fl_{N_R} [(gN Rubisco) (gN leaf)$^{-1}$]	smps_o (mm)	smps_c (mm)	$\text{rho}_{\text{vis,nir}}$	$\text{rho}_{\text{vis,nir}}$	$\text{tau}_{\text{vis,nir}}$	$\text{tau}_{\text{vis,nir}}$	$z_{0_{\text{mr}}}$	displa_r	d_{leaf} (m)
Ctrl	—	9.0	0.06	0.050	0.0	25.0	0.10	-7.74×10^4	-2.75×10^5	0.11, 0.58	0.36, 0.58	0.07, 0.25	0.22, 0.38	0.12	0.68	0.04
Sugar beet	118.0	6.7	0.062	0.020	0.0	10.0	0.15	-4.20×10^3	-1.65×10^5	0.10, 0.46	0.30, 0.46	0.09, 0.25	0.22, 0.78	0.12	0.68	0.28
Winter wheat	80.0	7.0	0.0476	0.028	0.0	14.0	0.3	-7.04×10^4	-1.60×10^5	0.10, 0.42	0.30, 0.42	0.08, 0.25	0.25, 0.95	0.13	0.70	0.05

transpiration rate (5 mm day^{-1} for the −3200 mm and 1 mm day^{-1} for −6000 mm), and smps_c is equal to −165 000 mm. The value of smps_o for winter wheat varies between −5000 and −9000 mm, depending on transpiration rate (5 mm day^{-1} for the −5000 mm and 1 mm day^{-1} for −9000 mm), and smps_c is set to −160 000 mm. The foliage nitrogen limiting factor remained unchanged and was set to 0.61 for both crops.

Optical properties of sugar beet and winter wheat were measured with a spectroradiometer (Field Spec Pro; ASD, Inc., Boulder, Colorado) coupled with the FluoWat leaf clip; methods are described in Van Wittenberghe et al. (2013). The resulting reflectance and transmittance values for the visible and near-infrared wave bands are given in Table 1. Roughness lengths for momentum transfer $z_{0_{\text{mr}}}$ and displacement heights displa_r were set to 0.12 and 0.68, as frequently reported for agricultural crops (Monteith and Unsworth 2013). Characteristic dimensions of fully expanded sugar beet and winter wheat leaves d_{leaf} were measured at different field locations with a caliper and measuring tape.

c. *Integrated Terrestrial Systems Modeling Platform*

TerrSysMP is a modular Terrestrial Systems Modeling Platform (Shrestha et al. 2014) that comprises the Consortium for Small-Scale Modeling (COSMO) numerical weather prediction model in a convection-permitting configuration (COSMO-DE; Baldauf et al. 2011), the CLM3.5 (Oleson et al. 2008), and the 3D variably saturated groundwater and surface water flow code ParFlow (Jones and Woodward 2001; Kollet and Maxwell 2006). The external coupler Ocean Atmosphere Sea Ice Soil, version 3 (OASIS3; Valcke 2013), is used to drive TerrSysMP and control the exchange of fluxes between each component model. The modeling platform can be configured to run with different combinations of component models: COSMO coupled with CLM3.5, CLM3.5 coupled with ParFlow (using offline atmospheric forcing), and the fully coupled system (COSMO–CLM3.5–ParFlow). Additionally, each model can be compiled and executed as a stand-alone independent model within TerrSysMP. The simulation results presented in this study were obtained running the stand-alone land surface component (CLM3.5) and the coupled atmosphere and land surface components (COSMO–CLM3.5); details about these two configurations are outlined in the following paragraph.

In TerrSysMP, the atmospheric forcing terms and the land surface fluxes are exchanged sequentially. The atmospheric state of COSMO at its lowest level and current time step (i.e., air temperature, wind speed, specific humidity, convective and grid-scale precipitation, pressure, incoming shortwave and longwave radiation, and

measurement height) forces CLM3.5, which in turn computes and sends back to COSMO the surface energy fluxes, momentum fluxes, albedo, and outgoing longwave radiation in an operator splitting approach. The dimensionless surface transfer coefficients of COSMO are subsequently updated with these fluxes, and the vertical gradients at the bottom level are calculated using the surface temperature from the previous time step. The new surface temperature and surface humidity are estimated based on the outgoing longwave radiation and latent heat flux, respectively. The computed direct and diffuse albedos and the outgoing longwave radiation are sent from CLM3.5 to COSMO as lower boundary conditions for the radiative transfer calculation. The exchange of fluxes can be performed by adopting different spatial and temporal resolutions for each independent component model by using time integration/averaging and spatial interpolation operators. These features, which include the downscaling of atmospheric state variables near the surface in response to land surface heterogeneity by Schomburg et al. (2010, 2012), allow for a scale-consistent coupling in the soil–vegetation–atmosphere continuum.

3. Results and discussion

a. *Validation of plant-specific parameterizations*

1) Model setup

Numerical simulations were performed with the land surface component of TerrSysMP (CLM3.5) using the crop-specific physiological parameterizations determined at the three measurement sites (Merken, Selhausen, and Merzenhausen). The runs were carried out at each test site using 2.8-km-resolution COSMO-DE reanalysis data (incoming shortwave and longwave radiation, temperature, precipitation, wind speed, pressure, and humidity) at an hourly time step over multiple years, namely, 2009, 2011, 2012, and 2013. The simulations were run at 1-h integration time steps with model results dumped at the same time frequency. Monthly leaf area index (LAI) was estimated by conducting a phenology study from 2002 to 2011 using the cloud-screened Moderate Resolution Imaging Spectroradiometer (MODIS, MCD15A2 product) 8-day composite from the *Aqua* and *Terra* satellites (Shrestha et al. 2014). Comparison between the estimated LAI values and occasional on-site measurements reveals a slight underestimation of the estimated leaf coverage in the postprocessed MODIS data. In the case of winter wheat, for instance, the LAI estimated for April is about 1.75; the corresponding sparse measurements give an averaged value of about 2.2. In the case of sugar beet, the estimated value for August is about 2.5, whereas the measurements indicate an LAI value around 3.3. The stem area index (SAI) was assessed based on LAI following Zeng et al. (2002) and Sellers et al. (1996). Information retrieved from the Food and Agriculture Organization of the United Nations Educational, Scientific and Cultural Organization (FAO-UNESCO) database (IUSS 2006) resulted in a soil texture composed of 35% clay and 35% loam. Soil color classification was adopted from information used in the operational version of the COSMO-DE model.

Two model configurations (ctrl crop vs sugar beet and/or ctrl crop vs winter wheat) were compared at each measurement station. Simulations were carried out during crop-specific growing seasons with sufficient observed data coverage. According to these constraints the following time periods were identified: in Merken, we selected the period from May to August 2009 for sugar beet; in Selhausen, from June to September 2011 for sugar beet; and in both Merzenhausen and Selhausen, from February to June for the years 2012 and 2013 for winter wheat. Finally, soil moisture and soil temperature of each model configuration were initialized by performing spinup runs, with CLM3.5 driven by reanalysis data and repeatedly reinitialized until dynamic equilibrium condition was reached.

2) Comparison of simulated energy fluxes

The performance of the different parameter sets in reproducing hourly latent and sensible heat were summarized using Taylor diagrams (Taylor 2001), which allow the simultaneous visualization of multiple statistical parameters (correlation, normalized standard deviation, and centered root-mean-square difference) between simulated and observed fluxes. Figure 2 shows the comparison between the ctrl crop and sugar beet plant functional type for the Merken and Selhausen (2011) measurement sites. The new parameter set (sugar beet) leads to a better agreement with observed values, with significant improvements in reproducing the amplitude of observed fluxes (normalized standard deviation σ_s/σ_o), and to a lesser extent, in reducing the centered root-mean-square difference. This is visible in the Taylor diagram by the positions of the points representing the sugar beet crop functional type in relation to the reference line ($\sigma_s/\sigma_o = 1$); the sugar beet points are closer to this reference line than the ctrl crop points. At the Merken site, for instance, the normalized standard deviation of the sensible heat changed from 2.0 (ctrl crop) to 0.75 (sugar beet), and from 0.5 (ctrl crop) to nearly 1.0 (sugar beet) for the latent heat. Correspondingly, at the Selhausen site, the normalized standard deviation of the latent heat increased from 0.5 (ctrl crop) to 0.8 (sugar beet) and decreased from 1.25 (ctrl crop) to 0.5 (sugar beet) for the sensible heat. In terms of phase, the results

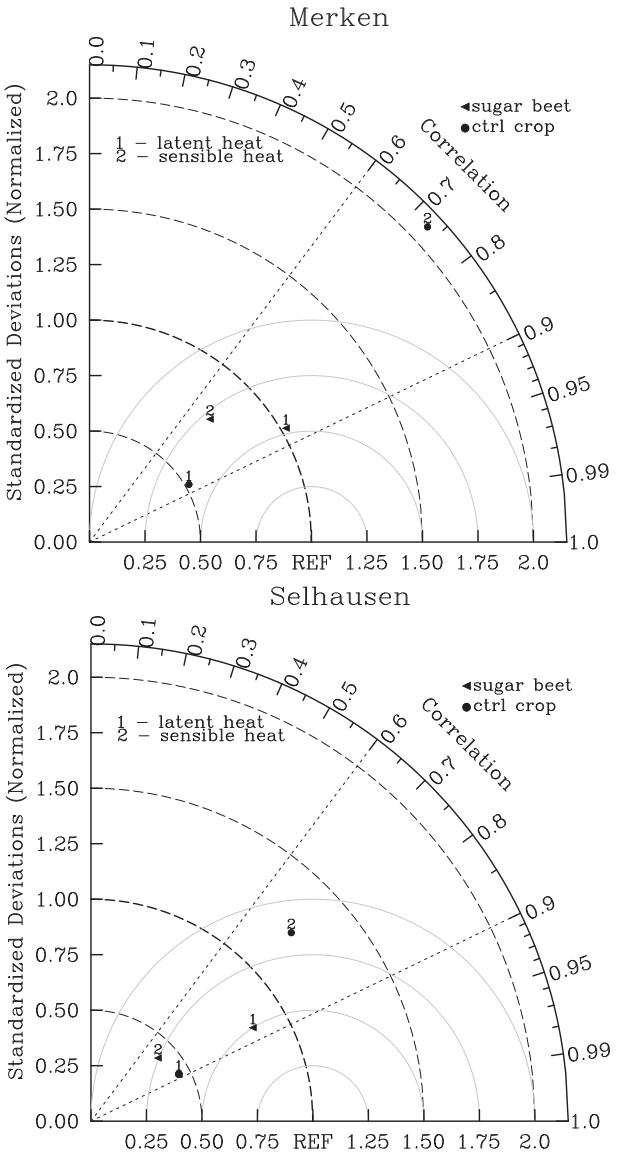

FIG. 2. Statistics of the hourly sensible and latent flux from the ctrl crop (circles) and sugar beet (triangles) for (top) Merken and (bottom) Selhausen measurement sites. The radial distance from the origin to the numbers is the std dev of the simulated hourly flux normalized by the std dev of the observations (σ_s/σ_o), with the REF line representing the observations. The azimuthal position of the numbers is the linear correlation between simulated and observed hourly flux.

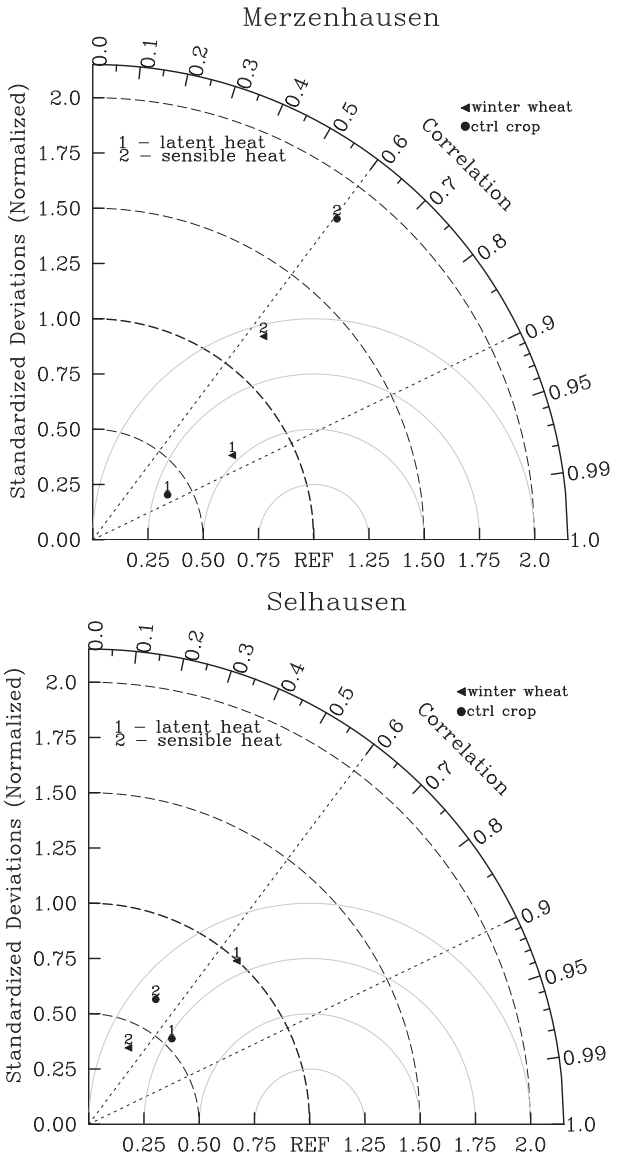

FIG. 3. Statistics of the hourly sensible and latent flux from the ctrl crop (circles) and winter wheat (triangles) for (top) Merzenhausen and (bottom) Selhausen measurement sites.

with the new parameters match well with the observations, with good correlations r for latent heat ($r = 0.86$ and $r = 0.87$ for Merken and Selhausen, respectively) and sensible heat ($r = 0.70$ and $r = 0.71$) that passed a Student's t test at the 95% confidence level. Similar improvements were noted for the winter wheat plant functional type at the Merzenhausen site (Fig. 3), where the normalized standard deviation of the latent and sensible heat fluxes improved by 25% and 75%, respectively, compared to ctrl crop. At the Selhausen site (2013), however, the improvement in the amplitude (50%) of the simulated latent heat flux was achieved along with an apparent deterioration (20%) of the simulated sensible heat. This is mainly an effect of the systematic underestimation of sensible heat flux during nighttime. Again, enhancements in the amplitude of the fluxes were obtained without degrading the phase of the simulated fluxes as indicated by the nearly unchanged correlation coefficients.

Despite improvements in the simulation of the energy fluxes, the new crop functional types still indicate some discrepancies with respect to the observed values related

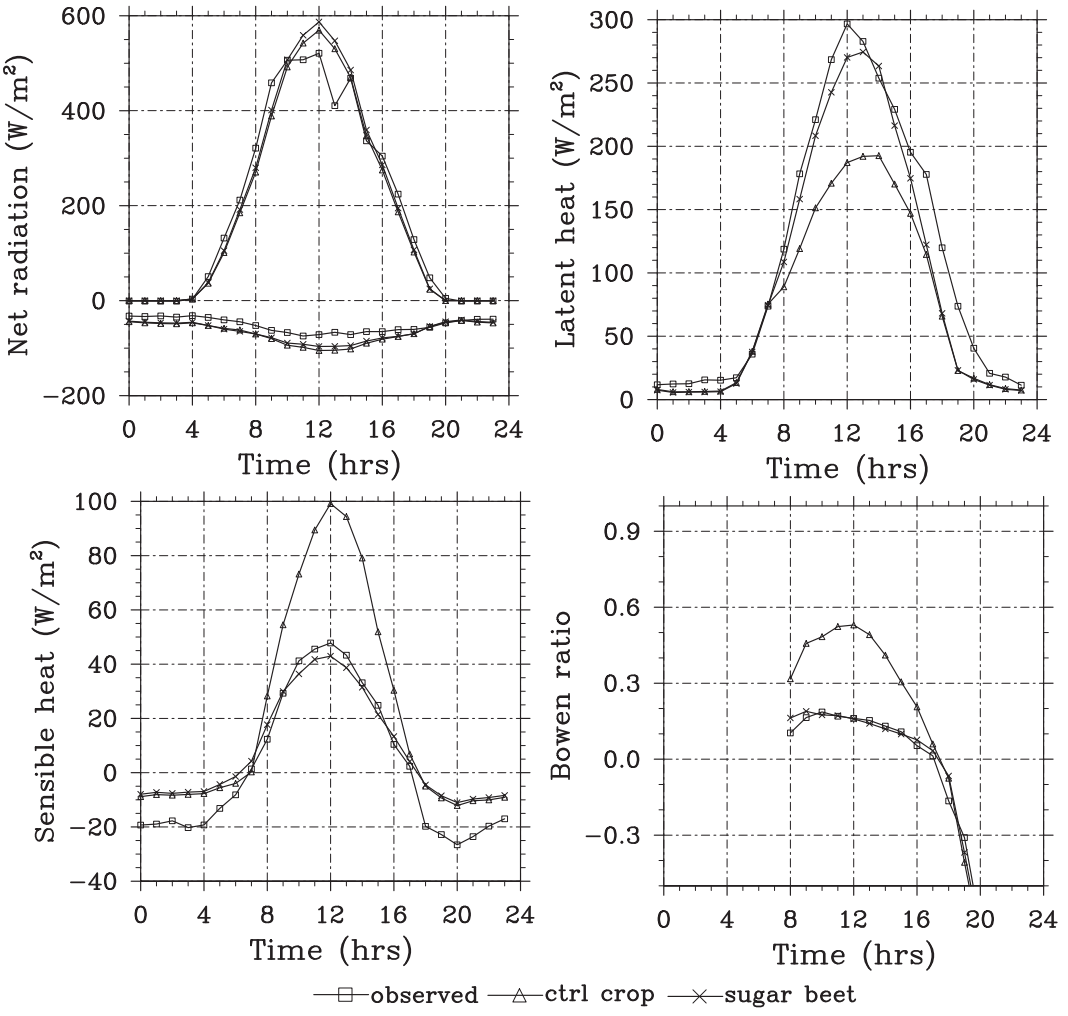

FIG. 4. Observed and simulated monthly averaged diurnal cycle of net shortwave (upper lines) and longwave (lower lines) (top left) radiation, (top right) latent heat, (bottom left) sensible heat, and (bottom right) Bowen ratio at the Selhausen site (June 2011).

to the components of the energy budget as simulated by the standard and new crop-specific parameter sets. To explain these discrepancies, we calculated the monthly averaged diurnal cycle of the radiation forcing terms, and the latent and sensible heat responses. Figure 4 shows the diurnal composites for June 2011 at the Selhausen site (sugar beet field) when eddy covariance and meteorological observations were both available. This analysis suggests an overestimation of the net radiation for both (standard and specific) crop configurations, possibly resulting from an underestimation of the albedo in combination with an overestimation (cloudiness effect) of incoming solar radiation in the coarse-resolution (2.8 km) reanalysis data used to force the land surface model. The net longwave radiation also exhibits a larger diurnal variation in the simulations. These discrepancies are slightly less when using the new crop-specific parameter set. It is important to note that errors in both radiation components tend to partially cancel each other, with the result that both model configurations capture the averaged diurnal variation of the net radiation term reasonably well. The influence of adopting an improved crop parameterization appears clearer in the analysis of the partitioning of net radiation into latent and sensible heat fluxes. Indeed, as illustrated in Fig. 4, the sugar beet plant functional type notably improves the magnitude of the simulated fluxes in favor of a higher latent heat flux and a lower sensible heat flux, which translates into more realistic (i.e., closer to observations) surface energy partitioning (evident from the Bowen ratio) for the new crop-specific parameter sets. The slight underestimation of the latent heat flux, shown also in Fig. 2 for the whole simulation period, could be explained by the lower LAI values estimated using the MODIS data as discussed in

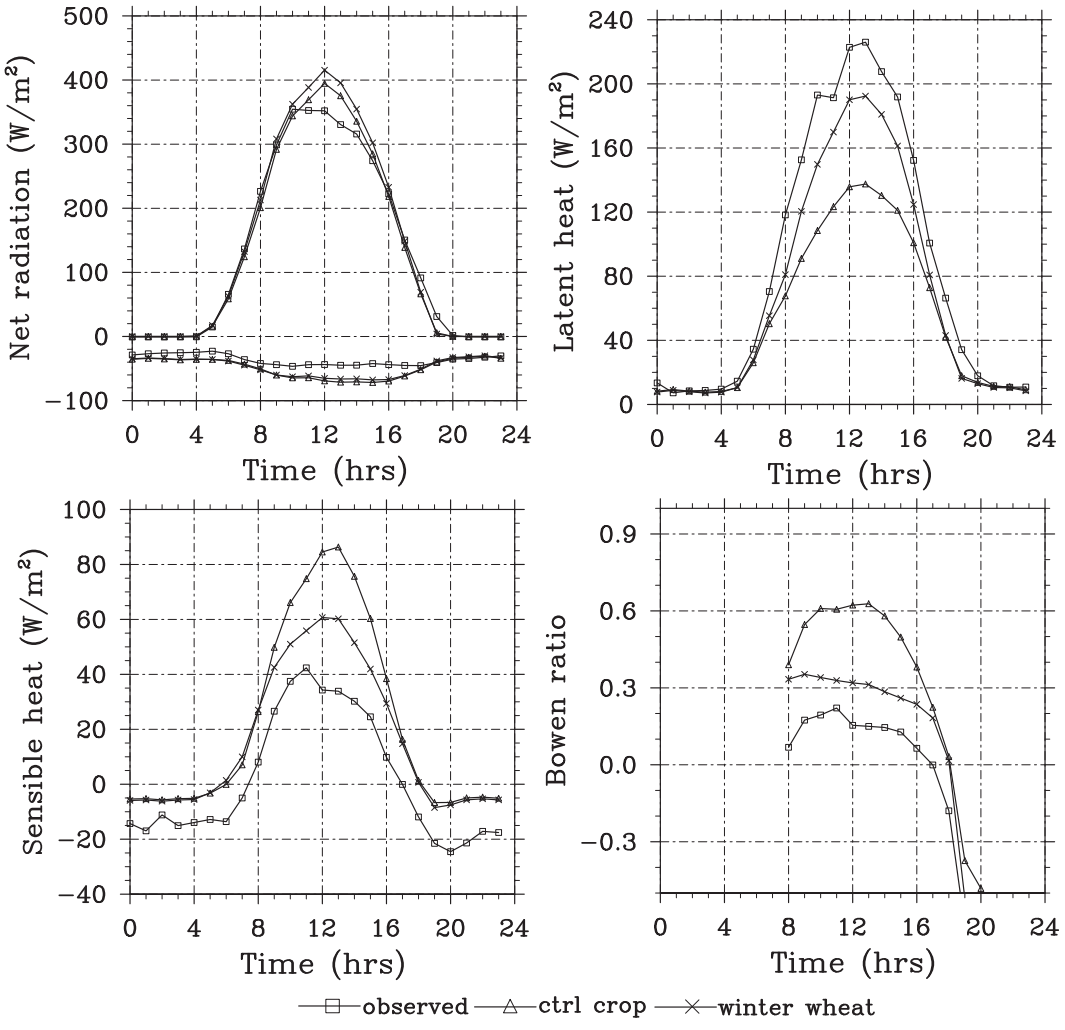

FIG. 5. Observed and simulated monthly averaged diurnal cycle of net shortwave (upper lines) and longwave (lower lines) (top left) radiation, (top right) latent heat, (bottom left) sensible heat, and (bottom right) Bowen ratio at the Selhausen site (May 2013).

section 3a(1). Note also that in the case of the sugar beet plant functional type, the difference between daytime observed and simulated surface energy fluxes (the sum of latent and sensible heat; LE + H) is about 12%, which is in the error range usually associated with eddy covariance measurements (Mauder et al. 2013). This discrepancy increases during the night when this technique is less reliable (Wilson et al. 2002).

The analysis of the monthly averaged energy budget components was also performed at the Selhausen measurement site (2013) for the winter wheat plant functional type. Again, the plant-specific parameter set results in a better agreement with the observations in terms of magnitude and partitioning of the energy fluxes at the land surface. This is shown in Fig. 5 using May 2013 as a representative month. In this comparison, for instance, the percent difference between simulated fluxes using the generic and crop-specific parameter sets is around 40%, the latter being closer to the observations. Some discrepancies, however, are still apparent in the different energy balance components, especially in the radiative components and in the sensible heat flux. It appears, indeed, that both model simulations (for generic and specific crop configurations) tend to overestimate the surface soil temperature, which is the reason for higher upward longwave radiation and higher sensible heat flux simulated during daytime compared to the observations. At nighttime, on the contrary, the higher values of simulated soil temperature cause a lower soil–atmosphere temperature gradient that in turn reduces the sensible heat flux. Finally, it is interesting to note that simulation results using the sugar beet and winter wheat parameter sets are closer than the results from each of them compared to those

obtained from the generic crop set. Because of data scarcity and crop rotation, this analysis was performed at the Selhausen and Merzenhausen field sites for June 2011. The observations and the simulated values (not shown here for the sake of brevity) show a 10% difference in the Bowen ratio between the winter wheat and sugar beet crops, with the latter experiencing slightly higher moisture fluxes. Further insights about the contrasting response of the two specific plant functional types on a daily time scale are outlined in section 3b(2).

3) Comparison of simulated carbon fluxes

Simulated fluxes were significantly improved by introducing a specific plant physiological parameterization (Figs. 2 and 3). Because latent heat and photosynthetic carbon uptake are constrained reciprocally, a complete validation of the proposed parameterizations also involves comparison between simulated and observed carbon fluxes. Figure 6 shows the monthly averaged values of gross primary production obtained from the flux partitioning described in section 2a for both the sugar beet (June 2011) and winter wheat (May 2013) crop at the Selhausen site. The analysis shows a significant increase in the simulated GPP for the two specific parameterizations, with a maximum diurnal cycle difference on the order of 25 μmol m^{-2} s^{-1}. This increase ultimately led to GPP overestimations of 6 μmol m^{-2} s^{-1} and underestimations of 8 μmol m^{-2} s^{-1} for the sugar beet and winter wheat crops, respectively. The close match in the simulated carbon fluxes clearly suggests that the enhanced model performance largely stems from an improved quantification of the photosynthesis process in the two specific crops, which is directly linked to the transpiration fluxes of the plant via the leaf stomatal resistance. It is also important to note that the relative ratio of maximum values of photosynthesis between the generic and specific crop parameterizations tends to be dampened in the maximum values of latent heat flux, shown in Figs. 4 and 5. This is mainly due to the gentler slope in the conductance-to-photosynthesis relationship mp, shown in Table 1 in the case of crop-specific parameterizations. This parameter is usually constant for all crop types (e.g., 9 in CLM3.5 and updated versions); however, experimental observations conducted in the study area showed a wide range of values between the analyzed crop species (e.g., 1.96–10.83 for sugar beet, 1.29–8.67 for winter wheat). This variability and the strong model sensitivity to mp (Prihodko et al. 2008; Göhler et al. 2013) emphasize the importance of implementing specific physiological characterizations for diverse crop species to accurately model heat and matter fluxes. Note also that the sugar beet plant functional type

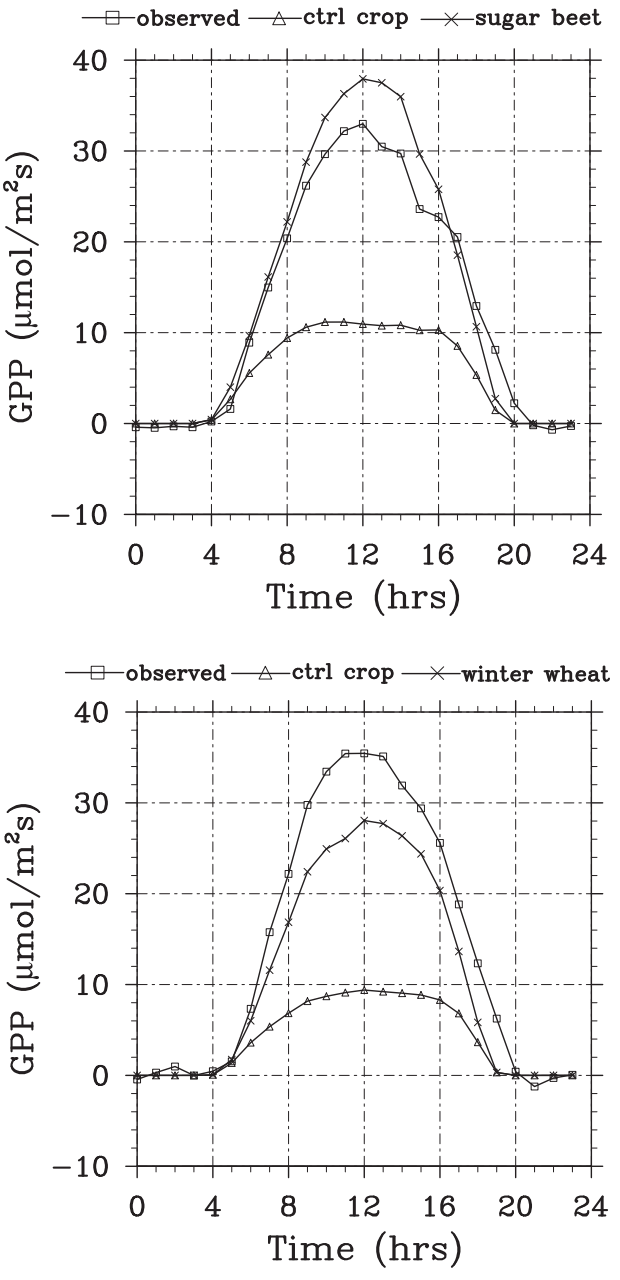

FIG. 6. Observed and simulated monthly averaged GPP diurnal cycle of (top) sugar beet in June 2011 and (bottom) winter wheat in May 2013 at the Selhausen site.

underestimates latent heat and overestimates photosynthesis fluxes. This opposite offset with respect to the measurements is probably related to estimation of daytime values of ecosystem respiration fluxes using air temperature instead of soil temperature.

An interpretation of these drastic improvements in the GPP requires an understanding of the model structure and its parameterization. In TerrSysMP (CLM3.5), photosynthesis is computed using a biogeochemical

approach (Sellers et al. 1996). It considers the stoichiometry of the leaf photosynthetic thylakoid electron transport, carbon reduction and oxidation cycles (von Caemmerer 2000), and scaling of the corresponding leaf-level photosynthesis model to the canopy by separately integrating its sunlit and shaded leaf fractions. In this approach, the photosynthetic rate limited by the Rubisco enzyme Vcmax is calculated using the model of Thornton and Zimmermann (2007) in which the area-based leaf nitrogen content is calculated from the leaf carbon to nitrogen ratio and the specific leaf area at the canopy top. Note here the notable difference in Table 1, especially for winter wheat, between the nitrogen concentration at the tissue level extracted from multiple measurements during the crop growing season and the value prescribed in the generic crop formulation. This difference is probably related to the fertilization activities in the crop fields that are not accounted for in the model parameterization. The strong control exhibited by $\text{leaf}_{\text{C:N}}$ has been demonstrated by White et al. (2000) in a factorial sensitivity analysis using a dynamic ecosystem model. In our work, this strong sensitivity was confirmed by implementing a much simpler one-factor-at-a-time approach, which showed a substantial increase of GPP with a decreasing $\text{leaf}_{\text{C:N}}$. The value of Vcmax is subsequently calculated by multiplying the area-based nitrogen content with the fraction of nitrogen in Rubisco, the mass ratio of total Rubisco molecular mass to nitrogen in Rubisco (set equal to 7.16), the specific activity of Rubisco, and accounting for temperature effects on metabolic processes and soil water limitation. As discussed in section 2b, the fraction of leaf nitrogen in Rubisco was derived from literature values, and the values, especially for winter wheat, are much different than those prescribed in the standard version of the land surface component CLM3.5 in TerrSysMP. The resulting Vcmax_{25} values show notable differences between the generic ctrl crop [21 (μmol CO_2) m^{-2} s^{-1}] and the specific sugar beet [196 (μmol CO_2) m^{-2} s^{-1}] and winter wheat [190 (μmol CO_2) m^{-2} s^{-1}] configurations. This large variability and its substantial effect on the improvement of simulated GPP (Bonan et al. 2011) suggest, as demonstrated also in previous investigations (Kattge et al. 2009; Chen et al. 2011) conducted by performing sensitivity and uncertainty analyses, that the usefulness of the proposed parameterization is based on a better representation of the vegetation nitrogen and catalytic effect of Rubisco on plant CO_2 uptake. Recent studies have also shown that these values are even cultivar specific (White 2009), highlighting the need for further improvements in land surface model parameterizations.

b. *Impact of plant-specific parameterizations on land–atmosphere interactions*

1) EXPERIMENT DESIGN

The influence of crop-specific physiological properties on land–atmosphere interactions was assessed by performing a series of numerical experiments over a geographical domain of 150 km × 150 km encompassing the North Rhine–Westphalia region, located in western Germany, Belgium, the Netherlands, and Luxembourg (Fig. 1). The experiments were carried out over a selected period of two consecutive clear-sky days (1–2 June 2011) using the coupled atmosphere–land surface (COSMO–CLM3.5) component of TerrSysMP. The atmospheric component uses a constant lateral spatial resolution of about 1 km and a variable vertical discretization into 50 levels gradually coarsening from the bottom (20 m) to the top (22 000 m). Land surface features were resolved with a higher horizontal resolution of 500 m in order to better represent the heterogeneous land-use information from the MODIS data (Shrestha et al. 2014). Bilinear (from the atmosphere to the land surface) and distance weighted (from the land surface to the atmosphere) interpolation methods were used to exchange fluxes and state variables between both model components. Time steps of 10 and 900 s were used for the atmospheric and land surface components, respectively, along with a coupling frequency of 900 s, which matches the frequency of radiation updates in the atmospheric model component. Atmospheric variables are averaged over this time period and sent to the land surface model. Initial and lateral boundary conditions for the atmospheric model were obtained from the operational weather forecast model COSMO-DE of the German Meteorological Service [Deutscher Wetterdienst (DWD)]. Initial soil moisture and soil temperature were obtained from spinup runs with the stand-alone land surface component (CLM3.5) of TerrSysMP, driven with reanalysis data and repeatedly reinitialized until dynamic equilibrium condition was reached. Three semi-idealized numerical experiments were performed by replacing the generic crop type (Fig. 1), which occupies 35% of the domain, with the sugar beet and winter wheat specific plant functional types.

2) MOISTURE AND HEAT BUDGETS OF THE ATMOSPHERIC BOUNDARY LAYER

We assessed the contrasting response of the ABL to the generic (ctrl crop) and specific (sugar beet and winter wheat) plant functional types using the concept of vector representation of the ABL heat and moisture budgets in the form of mixing diagrams (Betts 1992; Santanello et al.

2009). In this approach the diurnal coevolution of 2-m humidity q and potential temperature θ plotted as a 2D surface flux vector in the Lq–$C_p\theta$ plane are used to diagnose conditions and processes at the land surface and the top of the ABL, where L is the latent heat of vaporization and C_p is the specific heat. Specifically, the components (i.e., $L\Delta q$ and $C_p\Delta\theta$) of the surface flux vector are calculated integrating the latent and sensible heat over a diurnal interval, and calculating the average height of the ABL over the same time period. The contributions from the top of the boundary layer (i.e., the components of the entrainment flux vector) are estimated as a residual from the last state of temperature and humidity over the same time interval. Having derived the surface and the entrainment vectors (i.e., their components for sensible and latent heat), the relative contributions of bottom and top boundaries in the heat and moisture budgets can be quantified by a set of indices ($\beta_{\rm sfc} = H_{\rm sfc}/{\rm LE}_{\rm sfc}$, $\beta_{\rm ent} = H_{\rm ent}/{\rm LE}_{\rm ent}$, $A_H = H_{\rm ent}/H_{\rm sfc}$, and $A_{\rm LE} = {\rm LE}_{\rm ent}/{\rm LE}_{\rm sfc}$). These define the partitioning between latent and sensible heat β at the surface sfc and the entrainment ent interface, and the proportion of sensible and latent heat input A to the ABL from the two interfaces. For additional details about the graphical representation of the approach, the reader is referred to Santanello et al. (2009, 2011).

The observed and simulated diurnal coevolution of Lq and $C_p\theta$ on 2 June 2011, at the winter wheat (Merzenhausen) and sugar beet (Selhausen) measurement stations (Fig. 7) generally agree well at both sites. In particular for the winter wheat field the model nicely reproduces the decrease of q early in the afternoon due to dry air entrainment followed by an increase when the boundary layer growth ceases. A closer examination also reveals that the larger simulated amplitude in the moisture variations for the crop-specific parameter sets improves the match with the observed patterns. These diagrams also reveal a lower dynamic range and higher values of $C_p\theta$ (especially early in the morning) reproduced by the simulations (generic and specific crop parameterizations) with respect to the corresponding values measured at both sites. This is due to increased sensible heat caused by higher simulated soil temperature that tends to warm the lowest atmospheric level.

We further evaluate the effects of the different parameter sets on the energy partitioning indices defined above. As expected, at the Merzenhausen site (winter wheat), the computed surface and entrainment Bowen ratios confirm higher moistening of the boundary layer from the surface when using the crop-specific parameter set compared to the control set ($\beta_{\rm sfc,ctrl} = 0.73$ and $\beta_{\rm sfc,ww} = 0.20$) along with smaller variations between the two configurations in the ratio of dry air to heat being

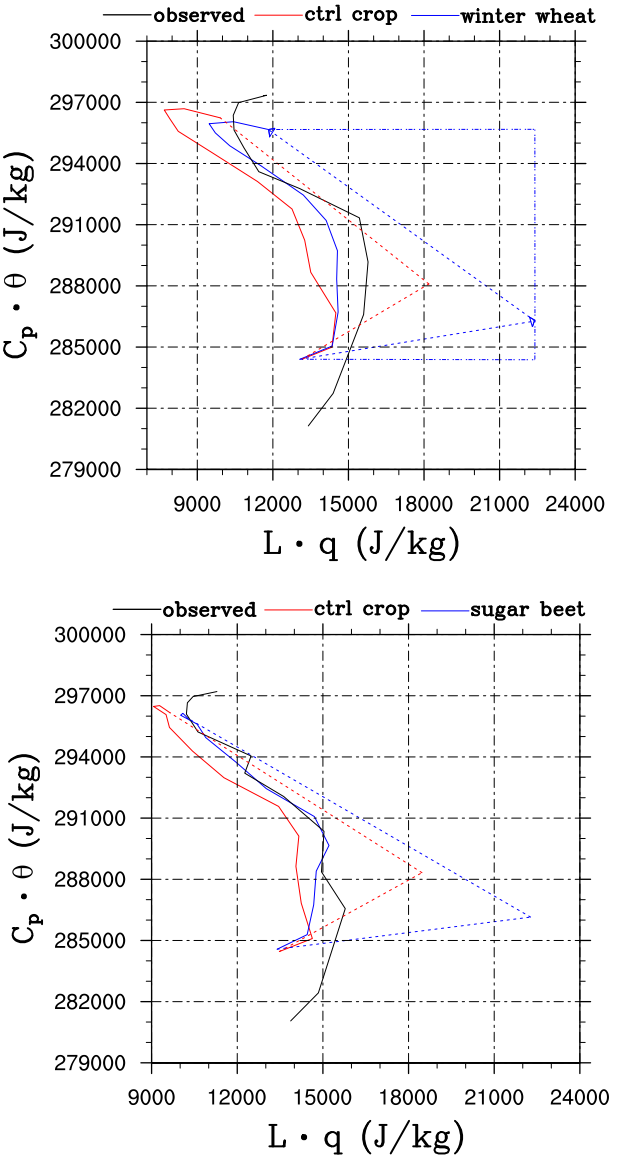

FIG. 7. Diurnal coevolution (0400–1600 UTC) of Lq and $C_p\theta$ on 2 Jun 2011 at the (top) Merzenhausen and (bottom) Selhausen site as observed (black line) and simulated [red line, ctrl crop; blue line, winter wheat in (top) and sugar beet in (bottom)]. The dashed lines indicate the surface ($\mathbf{V}_{\rm sfc}$) and entrainment vectors ($\mathbf{V}_{\rm ent}$), with the dash–dotted lines representing the heat (i.e., $C_p\Delta\theta$) and moisture (i.e., $L\Delta q$) component.

entrained ($\beta_{\rm ent,ctrl} = 0.98$ and $\beta_{\rm ent,ww} = 0.89$). The differences in land surface energy partitioning impact also the entrainment ratios ($A_{H_{\rm ctrl}} = 2.21$, $A_{H_{\rm ww}} = 5.01$, $A_{{\rm LE}_{\rm ctrl}} = -1.64$, and $A_{{\rm LE}_{\rm ww}} = -1.13$), with a larger A_H for the crop-specific parameter set indicating the increased control of entrainment heat fluxes over the surface fluxes. Note also that, for the case of winter wheat, $A_{\rm LE}$ tends to -1.0, that is, a closer balance between the surface and the entrainment moisture fluxes. The lower surface sensible heat simulated

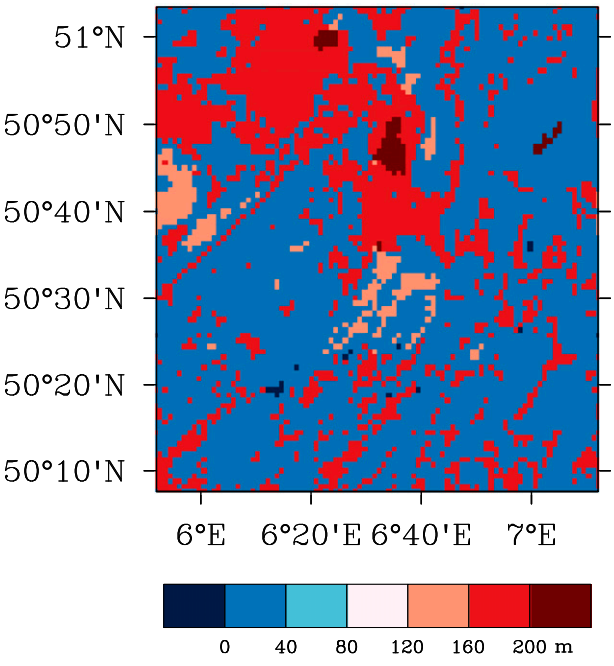

FIG. 8. ABL height difference between ctrl crop and winter wheat. The positive values indicate that ABL heights were lower for the winter wheat than the ctrl crop run. The snapshot was obtained at 1000 UTC 2 Jun 2011.

by the winter wheat parameter set results in a shallower ABL (by 100–350 m), compared to the control crop configuration. Figure 8 shows a snapshot of the spatial distribution of the ABL height differences inside the domain depicted in Fig. 1, which clearly follows the distribution of the land-use classes with maximum values located in the northern part dominated by crops.

A similar response was found at the Selhausen site (sugar beet) in terms of Bowen ($\beta_{\mathrm{sfc,ctrl}} = 0.77$, $\beta_{\mathrm{sfc,sb}} = 0.18$, $\beta_{\mathrm{ent,ctrl}} = 0.89$, and $\beta_{\mathrm{ent,sb}} = 0.82$) and entrainment ratios ($A_{H_{\mathrm{ctrl}}} = 2.03$, $A_{H_{\mathrm{sb}}} = 6.24$, $A_{\mathrm{LE}_{\mathrm{ctrl}}} = -1.77$, and $A_{\mathrm{LE}_{\mathrm{sb}}} = -1.35$). Compared to the winter wheat, the simulations with control and crop-specific parameter sets have larger differences (~10%) in surface energy partitioning, with the sugar beet plant functional type leading to higher latent heat fluxes with respect to the ctrl crop. Accordingly, the top fluxes contribute more to the heat budget of the ABL. Differences between model-calculated heights of the ABL reach a maximum of about 300 m, with the sugar beet configuration simulating a shallower vertical extent. The spatial distributions of these differences are very similar to the ones shown for winter wheat and thus are not displayed here.

To further explore the influence of crop physiological properties on the ABL evolution, we analyzed the spatial distribution of potential temperature along the transect depicted in Fig. 1. The differences (ctrl crop–winter wheat and ctrl crop–sugar beet) along the south–north cross section are displayed in Fig. 9. The discontinuities in the atmosphere nicely align with the heterogeneity in land use along the transect, with a moister and cooler ABL simulated by the crop-specific parameter sets. Subtle but significant differences exist between the results of the two crop-specific parameter sets. At the latitude range 50°40′–50°65′N, the higher latent heat flux simulated by the winter wheat configuration leads overall to a cooler ABL and a warmer entrainment zone. The inverse situation can be found further to the north (50°80′–51°05′N), where the effect of higher moisture fluxes simulated by the sugar beet configuration result in a slightly cooler ABL and warmer entrainment zone. The opposite crop response is due to different soil conditions in that region, and point out the complex nonlinear interactions of plant physiological properties within the soil–vegetation–atmospheric continuum.

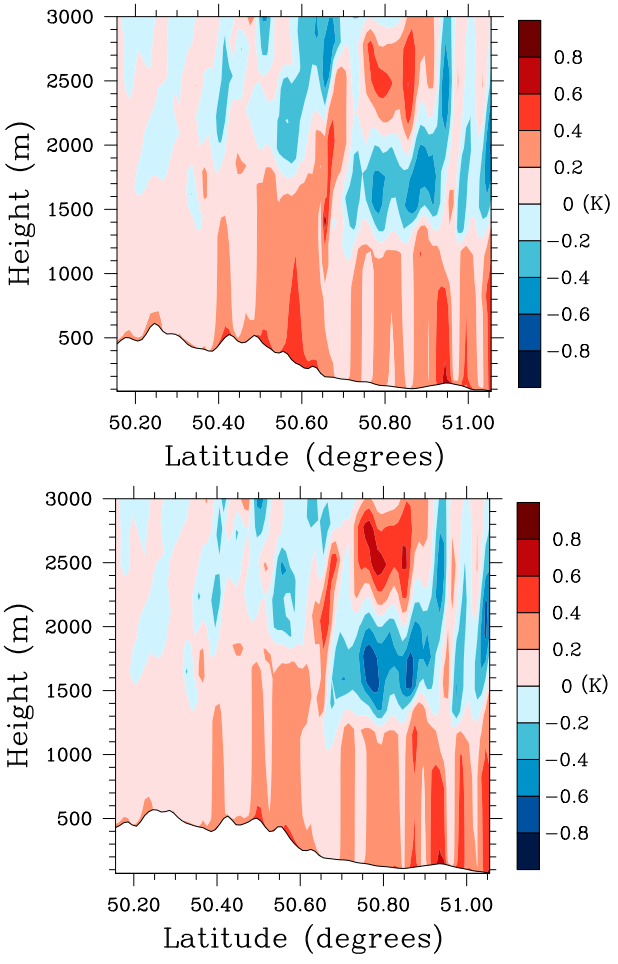

FIG. 9. South–north cross section depicted in Fig. 1 of the potential temperature difference between (top) ctrl crop and winter wheat and (bottom) crtl crop and sugar beet configurations. The cross sections were obtained at 1300 UTC 2 Jun 2011.

4. Summary and conclusions

This study investigated the influence of crop-specific physiological properties on the partitioning of land surface energy fluxes, and on the resulting modifications in the heat and moisture budgets of the ABL. To this aim, a set of physiological parameters describing the photosynthesis, optical, and aerodynamic properties of two crops, sugar beet and winter wheat, were retrieved from measurement campaigns carried out in an agricultural district of the North Rhine–Westphalia region of Germany. The crop-specific parameters were included in the biophysical component of a Terrestrial Systems Modeling Platform (TerrSysMP). Simulation runs were conducted to validate this new set of parameters against eddy covariance (sensible heat, latent heat, and CO_2) measurements, and to evaluate the improvements with respect to a generic crop parameterization. In addition, a set of atmosphere–land surface coupled numerical experiments were performed to assess the impact of this detailed plant characterization on the modeling of land–atmosphere interactions. These semi-idealized runs were designed by replacing the generic crop land use with the sugar beet and winter wheat parameterization over the North Rhine–Westphalia domain of Germany.

For the investigated region, the results show significant improvements in the simulated land surface heat and water fluxes when the generic CLM3.5 crop type is replaced by crop-specific physiological parameter sets. Simulations with parameter sets specific for sugar beet and winter wheat result in higher latent heat and lower sensible heat fluxes compared to the generic crop, which also better match with local eddy covariance measurements. An analysis of the diurnal energy cycle also reveals that despite some mismatch in the net radiation due to uncertainties in the atmospheric forcing term and the soil parameterization, the specific physiological properties of the plants reproduce well the observed diurnal partitioning between sensible and latent heat. These enhancements are corroborated by a comparison between simulated and observed carbon fluxes (GPP); here also the sugar beet and winter wheat parameter sets reproduce significantly higher CO_2 plant uptake than the generic crop in accordance with the observations. The latter result identifies the parameters controlling the Rubisco enzyme kinematics, and hence the photosynthesis process, as the main cause for the improvements.

The simulations performed using the land surface–atmosphere coupled components of TerrSysMP (COSMO–CLM3.5) reveal the influence of the adjusted physiological parameterizations on the heat and moisture budgets of the ABL. A mixing-diagram approach quantifies the wetting and cooling effect of the crop-specific parameter sets on the ABL compared to the generic crop parameterization. The resulting changes in the land surface energy partitioning translate, especially in the case of sugar beet, into a larger contribution of the entrainment zone to the heat budget of the ABL and to a shallower ABL. Results based on idealized configurations of the real domain underscore the importance of using crop-specific physiological properties for an improved modeling of land–atmosphere interactions. High-resolution spatial information of diverse crop species and associated physiological characterizations are therefore needed for an accurate simulation of the ABL evolution.

The detailed characterization of the large variety of crop species remains a great challenge for regional and continental applications; thus more generalized biome or plant functional type parameterizations are still used extensively. Advanced statistical techniques (e.g., adjoint methods; Schwinger et al. 2010) and extended observational networks represent a prime approach to infer optimal parameter combinations as well as to gain insight into model parameter sensitivity, uncertainty, and limitations. Advanced airborne sensors (e.g., HyPlant) in tandem with in situ measurements should be exploited for the derivation of specific physiological properties of the wide variety of crops. In this context, it must be noted that these properties, also termed as phenotype characteristics (Fiorani and Schurr 2013), do not remain constant both during a season and in between years. Underlying mechanisms due to different genetics have been understood for a while, but an integrated quantification of their effects remains a paramount challenge because of the extreme complexity of plant metabolic networks (Humbert et al. 2013). Noise found in the plant functional type parameters is partly caused by this phenomenon. Another reason is the lack of standardization of measurement approaches, which makes plant functional type values reported in the literature hardly comparable. Initiatives like the Australian PrometheusWiki (Sack et al. 2010) are commendable efforts to alleviate this problem. The presented work is part of a joint effort that seeks to incorporate detailed crop information into an integrated terrestrial modeling platform for a high-resolution representation of patterns and structures in the soil–vegetation–atmosphere continuum (Simmer et al. 2015). This attempt will eventually contribute to the community effort [e.g., Agricultural Model Intercomparison and Improvement Project (AgMIP)] for an improved understanding of cropland ecosystem feedbacks to long-term climate simulations.

Acknowledgments. This research work was supported by the SFB/TR32 Patterns in Soil–Vegetation–Atmosphere

Systems: Monitoring, Modeling and Data Assimilation project funded by the Deutsche Forschungsgemeinschaft (DFG). We thank Marius Schmidt and Alexander Graf for providing us with meteorological and flux data from the Eifel–Lower Rhine valley observatory of the TERENO project funded by the Helmholtz Association. We are grateful to Mostaquimur Rahman and John Williams for their valuable comments on an early version of the manuscript. We also thank the three anonymous reviewers for their detailed and helpful comments.

REFERENCES

Arora, V. K., 2002: Modeling vegetation as a dynamic component in soil–vegetation–atmosphere transfer schemes and hydrological models. *Rev. Geophys.,* **40,** 1006, doi:10.1029/2001RG000103.

——, 2003: Simulating energy and carbon fluxes over winter wheat using coupled land surface and terrestrial ecosystem models. *Agric. For. Meteor.,* **118,** 21–47, doi:10.1016/S0168-1923(03)00073-X.

Aubinet, M., C. Moureaux, B. Bodson, D. Dufranne, B. Heinesch, M. Suleau, F. Vancutsem, and A. Vilret, 2009: Carbon sequestration by a crop over a 4-year sugar beet/winter wheat/seed potato/winter wheat rotation cycle. *Agric. For. Meteor.,* **149,** 407–418, doi:10.1016/j.agrformet.2008.09.003.

Baldauf, M., A. Seifert, J. Förstner, D. Majewski, M. Raschendorfer, and T. Reinhardt, 2011: Operational convective-scale numerical weather prediction with the COSMO model: Description and sensitivities. *Mon. Wea. Rev.,* **139,** 3887–3905, doi:10.1175/MWR-D-10-05013.1.

Baldocchi, D., 1994: A comparative study of mass and energy exchange rates over a closed C_3 (wheat) and an open C_4 (corn) crop: II. CO_2 exchange and water use efficiency. *Agric. For. Meteor.,* **67,** 291–321, doi:10.1016/0168-1923(94)90008-6.

Ball, J. T., I. E. Woodrow, and J. A. Berry, 1987: A model predicting stomatal conductance and its contribution to the control of photosynthesis under different environmental conditions. *Progress in Photosynthesis Research,* J. Biggens, Ed., Springer, 221–224.

Betts, A. K., 1992: FIFE atmospheric boundary layer budget methods. *J. Geophys. Res.,* **97,** 18 523–18 532, doi:10.1029/91JD03172.

Betts, R. A., P. M. Cox, S. L. Lee, and F. I. Woodward, 1997: Contrasting physiological and structural vegetation feedbacks in climate change simulations. *Nature,* **387,** 796–799, doi:10.1038/42924.

Bonan, G. B., S. Levis, L. Kergoat, and K. W. Oleson, 2002: Landscapes as patches of plant functional types: An integrating concept for climate and ecosystem models. *Global Biogeochem. Cycles,* **16,** 1021, doi:10.1029/2000GB001360.

——, P. J. Lawrence, K. W. Oleson, S. Levis, M. Jung, M. Reichstein, D. M. Lawrence, and S. C. Swenson, 2011: Improving canopy processes in the Community Land Model version 4 (CLM4) using global flux fields empirically inferred from FLUXNET data. *J. Geophys. Res.,* **116,** G02014, doi:10.1029/2010JG001593.

——, K. W. Oleson, R. A. Fisher, G. Lasslop, and M. Reichstein, 2012: Reconciling leaf physiological traits and canopy flux data: Use of the TRY and FLUXNET databases in the Community Land Model version 4. *J. Geophys. Res.,* **117,** G02026, doi:10.1029/2011JG001913.

Bondeau, A., and Coauthors, 2007: Modelling the role of agriculture for the 20th century global terrestrial carbon balance. *Global Change Biol.,* **13,** 679–706, doi:10.1111/j.1365-2486.2006.01305.x.

Buckley, T. N., 2005: The control of stomata by water balance. *New Phytol.,* **168,** 275–292, doi:10.1111/j.1469-8137.2005.01543.x.

Chen, H., R. E. Dickinson, Y. Dai, and L. Zhou, 2011: Sensitivity of simulated terrestrial carbon assimilation and canopy transpiration to different stomatal conductance and carbon assimilation schemes. *Climate Dyn.,* **36,** 1037–1054, doi:10.1007/s00382-010-0741-2.

Davin, E. L., and N. de Noblet-Ducoudré, 2010: Climatic impact of global-scale deforestation: Radiative versus nonradiative processes. *J. Climate,* **23,** 97–112, doi:10.1175/2009JCLI3102.1.

de Noblet-Ducoudré, N., S. Gervois, P. Ciais, N. Viovy, N. Brisson, B. Seguin, and A. Perrier, 2004: Coupling the Soil–Vegetation–Atmosphere–Transfer Scheme ORCHIDEE to the agronomy model STICS to study the influence of croplands on the European carbon and water budgets. *Agronomie,* **24,** 397–407, doi:10.1051/agro:2004038.

Douville, H., S. Planton, J.-F. Royer, D. B. Stephenson, S. Tyteca, L. Kergoat, S. Lafont, and R. A. Betts, 2000: Importance of vegetation feedbacks in doubled-CO_2 climate experiments. *J. Geophys. Res.,* **105,** 14 841–14 861, doi:10.1029/1999JD901086.

Fiorani, F., and U. Schurr, 2013: Future scenarios for plant phenotyping. *Annu. Rev. Plant Biol.,* **64,** 267–291, doi:10.1146/annurev-arplant-050312-120137.

Foley, A., and Coauthors, 2005: Global consequences of land use. *Science,* **309,** 570–574, doi:10.1126/science.1111772.

Franks, P. J., P. L. Drake, and R. H. Froend, 2007: Anisohydric but isohydrodynamic: Seasonally constant plant water potential gradient explained by a stomatal control mechanism incorporating variable plant hydraulic conductance. *Plant Cell Environ.,* **30,** 19–30, doi:10.1111/j.1365-3040.2006.01600.x.

Friend, A. D., and Coauthors, 2007: FLUXNET and modelling the global carbon cycle. *Global Change Biol.,* **13,** 610–633, doi:10.1111/j.1365-2486.2006.01223.x.

Garcia-Carreras, L., D. J. Parker, C. M. Taylor, C. E. Reeves, and J. G. Murphy, 2010: Impact of mesoscale vegetation heterogeneities on the dynamical and thermodynamic properties of the planetary boundary layer. *J. Geophys. Res.,* **115,** D03102, doi:10.1029/2009JD012811.

Gayler, S., J. Ingwersen, E. Priesack, T. Wöhling, V. Wulfmeyer, and T. Streck, 2013: Assessing the relevance of subsurface processes for the simulation of evapotranspiration and soil moisture dynamics with CLM3.5: Comparison with field data and crop model simulations. *Environ. Earth Sci.,* **69,** 415–427, doi:10.1007/s12665-013-2309-z.

——, and Coauthors, 2014: Incorporating dynamic root growth enhances the performance of Noah-MP at two contrasting winter wheat field sites. *Water Resour. Res.,* **50,** 1337–1356, doi:10.1002/2013WR014634.

Georgescu, M., G. Miguez-Macho, L. T. Steyaert, and C. P. Weaver, 2009: Climatic effects of 30 years of landscape change over the greater Phoenix, Arizona, region: 1. Surface energy budget changes. *J. Geophys. Res.,* **114,** D05110, doi:10.1029/2008JD010745.

Göhler, M., J. Mai, and M. Cuntz, 2013: Use of eigendecomposition in a parameter sensitivity analysis of the Community Land Model. *J. Geophys. Res. Biogeosci.,* **118,** 904–921, doi:10.1002/jgrg.20072.

Graf, A., J. Werner, M. Langensiepen, A. van de Boer, M. Schmidt, M. Kupisch, and H. Vereecken, 2013: Validation of a minimum

microclimate disturbance chamber for net ecosystem flux measurements. *Agric. For. Meteor.,* **174–175,** 1–14, doi:10.1016/j.agrformet.2013.02.001.

Haugland, M. J., and K. C. Crawford, 2005: The diurnal cycle of land–atmosphere interactions across Oklahoma's winter wheat belt. *Mon. Wea. Rev.,* **133,** 120–130, doi:10.1175/MWR-2842.1.

Hay, R. K. M., and J. R. Porter, 2006: *The Physiology of Crop Yield*. Blackwell Publishing, 330 pp.

Humbert, S., S. Subedi, J. Cohn, B. Zeng, Y. M. Bi, and X. Chen, 2013: Genome-wide expression profiling of maize in response to individual and combined water and nitrogen stresses. *BMC Genomics,* **14,** doi:10.1186/1471-2164-14-3.

Ingwersen, J., and Coauthors, 2011: Comparison of Noah simulations with eddy covariance and soil water measurements at a winter wheat stand. *Agric. For. Meteor.,* **151,** 345–355, doi:10.1016/j.agrformet.2010.11.010.

IUSS, 2006: World Reference Base for Soil Resources 2006. FAO Tech. Rep. 103, 128 pp.

Jones, J. E., and C. S. Woodward, 2001: Newton–Krylov-multigrid solvers for large-scale, highly heterogeneous, variably saturated flow problems. *Adv. Water Resour.,* **24,** 763–774, doi:10.1016/S0309-1708(00)00075-0.

Kattge, J., W. Knorr, T. Raddatz, and C. Wirth, 2009: Quantifying photosynthetic capacity and its relationship to leaf nitrogen content for global-scale terrestrial biosphere models. *Global Change Biol.,* **15,** 976–991, doi:10.1111/j.1365-2486.2008.01744.x.

Kollet, S. J., and R. M. Maxwell, 2006: Integrated surface–groundwater flow modeling: A free-surface overland flow boundary condition in a parallel groundwater flow model. *Adv. Water Resour.,* **29,** 945–958, doi:10.1016/j.advwatres.2005.08.006.

Kothavala, Z., M. A. Arain, T. A. Black, and D. Verseghy, 2005: The simulation of energy, water vapor and carbon dioxide fluxes over common crops by the Canadian Land Surface Scheme (CLASS). *Agric. For. Meteor.,* **133,** 89–108, doi:10.1016/j.agrformet.2005.08.007.

Kucharik, C. J., and Coauthors, 2000: Testing the performance of a dynamic global ecosystem model: Water balance, carbon balance, and vegetation structure. *Global Biogeochem. Cycles,* **14,** 795–825, doi:10.1029/1999GB001138.

Kueppers, L. M., M. S. Snyder, and L. C. Sloan, 2007: Irrigation cooling effect: Regional climate forcing by land-use change. *Geophys. Res. Lett.,* **34,** L03703, doi:10.1029/2006GL028679.

Lawlor, D. W., 2002: Carbon and nitrogen assimilation in relation to yield: Mechanisms are the key to understanding production systems. *J. Exp. Bot.,* **53,** 773–787, doi:10.1093/jexbot/53.370.773.

Levis, S., G. B. Bonan, E. Kluzek, P. E. Thornton, A. Jones, W. J. Sacks, and C. J. Kucharik, 2012: Interactive crop management in the Community Earth System Model (CESM1): Seasonal influences on land–atmosphere fluxes. *J. Climate,* **25,** 4839–4859, doi:10.1175/JCLI-D-11-00446.1.

Lloyd, J., and J. A. Taylor, 1994: On the temperature dependence of soil respiration. *Funct. Ecol.,* **8,** 315–323, doi:10.2307/2389824.

Lu, X., Y.-P. Wang, T. Ziehn, and Y. Dai, 2013: An efficient method for global parameter sensitivity analysis and its applications to the Australian community land surface model (CABLE). *Agric. For. Meteor.,* **182–183,** 292–303, doi:10.1016/j.agrformet.2013.04.003.

Mahecha, M. D., and Coauthors, 2010: Comparing observations and process-based simulations of biosphere–atmosphere exchanges on multiple timescale. *J. Geophys. Res.,* **115,** G02003, doi:10.1029/2009JG001016.

Mauder, M., M. Cuntz, C. Drüe, A. Graf, C. Rebmann, H. P. Schmid, M. Schmidt, and R. Steinbrecher, 2013: A strategy for quality and uncertainty assessment of long-term eddy-covariance measurements. *Agric. For. Meteor.,* **169,** 122–135, doi:10.1016/j.agrformet.2012.09.006.

McPherson, R. A., and D. J. Stensrud, 2005: Influences of a winter wheat belt on the evolution of the boundary layer. *Mon. Wea. Rev.,* **133,** 2178–2199, doi:10.1175/MWR2968.1.

——, ——, and K. C. Crawford, 2004: The impact of Oklahoma's winter wheat belt on the mesoscale environment. *Mon. Wea. Rev.,* **132,** 405–421, doi:10.1175/1520-0493(2004)132<0405:TIOOWW>2.0.CO;2.

Monteith, J., and M. Unsworth, 2013: *Principles of Environmental Physics*. Academic Press, 422 pp.

Morales, P., and Coauthors, 2005: Comparing and evaluating process-based ecosystem model predictions of carbon and water fluxes in major European forest biomes. *Global Change Biol.,* **11,** 2211–2233, doi:10.1111/j.1365-2486.2005.01036.x.

Moureaux, C., A. Debacq, B. Bodson, B. Heinesch, and M. Aubinet, 2006: Annual net ecosystem carbon exchange by a sugar beet crop. *Agric. For. Meteor.,* **139,** 25–39, doi:10.1016/j.agrformet.2006.05.009.

Nemani, R., and S. W. Running, 1996: Implementation of a hierarchical global vegetation classification in ecosystem function models. *J. Veg. Sci.,* **7,** 337–346, doi:10.2307/3236277.

Niu, G.-Y., and Coauthors, 2011: The community Noah land surface model with multiparameterization options (Noah-MP): 1. Model description and evaluation with local-scale measurements. *J. Geophys. Res.,* **116,** D12109, doi:10.1029/2010JD015139.

Oleson, K. W., and Coauthors, 2008: Improvements to the Community Land Model and their impact on the hydrological cycle. *J. Geophys. Res.,* **113,** G01021, doi:10.1029/2007JG000563.

Pielke, R. A., 2001: Influence of the spatial distribution of vegetation and soils on the prediction of cumulus convective rainfall. *Rev. Geophys.,* **39,** 151–177, doi:10.1029/1999RG000072.

Prihodko, L., A. Denning, N. Hanan, I. Baker, and K. Davis, 2008: Sensitivity, uncertainty and time dependence of parameters in a complex land surface model. *Agric. For. Meteor.,* **148,** 268–287, doi:10.1016/j.agrformet.2007.08.006.

Raab, T. K., and T. Norman, 1994: Nitrogen source regulation of growth and photosynthesis in *Beta vulgaris L. Plant Physiol.,* **105,** 1159–1166.

Reynolds, O., 1894: On the dynamical theory of incompressible viscous fluid and the determination of the criterion. *Proc. Roy. Soc. London,* **56A,** 40–45, doi:10.1098/rspl.1894.0075.

Richardson, A. D., and D. Y. Hollinger, 2005: Statistical modeling of ecosystem respiration using eddy covariance data: Maximum likelihood parameter estimation, and Monte Carlo simulation of model and parameter uncertainty, applied to three simple models. *Agric. For. Meteor.,* **131,** 191–208, doi:10.1016/j.agrformet.2005.05.008.

Sack, L., W. K. Cornwell, L. S. Santiago, M. M. Barbour, B. Choat, J. R. Evans, R. Munns, and A. Nicotra, 2010: A unique web resource for physiology, ecology and the environmental sciences: PrometheusWiki. *Funct. Plant Biol.,* **37,** 687–693, doi:10.1071/FP10097.

Santanello, J. A., C. D. Peters-Lidard, S. V. Kumar, C. Alonge, and W. K. Tao, 2009: A modeling and observational framework for diagnosing local land–atmosphere coupling on diurnal time scales. *J. Hydrometeor.,* **10,** 577–599, doi:10.1175/2009JHM1066.1.

——, ——, and ——, 2011: Diagnosing the sensitivity of local land–atmosphere coupling via the soil moisture–boundary layer interaction. *J. Hydrometeor.,* **12,** 766–786, doi:10.1175/JHM-D-10-05014.1.

Schickling, A., and Coauthors, 2010: The influence of leaf photosynthetic efficiency and stomatal closure on canopy carbon uptake and evapotranspiration—A model study in wheat and sugar beet. *Biogeosci. Discuss.,* **7,** 7131–7172, doi:10.5194/bgd-7-7131-2010.

Schomburg, A., V. Venema, R. Lindau, F. Ament, and C. Simmer, 2010: A downscaling scheme for atmospheric variables to drive soil–vegetation–atmosphere transfer models. *Tellus,* **62** (4), 242–258, doi:10.1111/j.1600-0889.2010.00466.x.

——, ——, F. Ament, and C. Simmer, 2012: Disaggregation of screen-level variables in a numerical weather prediction model with an explicit simulation of subgrid-scale land-surface heterogeneity. *Meteor. Atmos. Phys.,* **116,** 81–94, doi:10.1007/s00703-012-0183-y.

Schulze, E.-D., F. M. Kelliher, C. Korner, J. Lloyd, and L. Ray, 1994: Relationships among maximum stomatal conductance, ecosystem surface conductance, carbon assimilation rate, and plant nitrogen nutrition: A global ecology scaling exercise. *Annu. Rev. Ecol. Syst.,* **25,** 629–660, doi:10.1146/annurev.es.25.110194.003213.

Schwinger, J., S. J. Kollet, C. Hoppe, and H. Elbern, 2010: Sensitivity of latent heat fluxes to initial values and parameters of a land-surface model. *Vadose Zone J.,* **9,** 984–1001, doi:10.2136/vzj2009.0190.

Sellers, P. J., S. O. Los, C. J. Tucker, C. O. Justice, D. A. Dazlich, G. J. Collatz, and D. A. Randall, 1996: A revised land surface parameterization (SiB2) for atmospheric GCMs. Part II: The generation of global fields of terrestrial biophysical parameters from satellite data. *J. Climate,* **9,** 706–737, doi:10.1175/1520-0442(1996)009<0706:ARLSPF>2.0.CO;2.

Shrestha, P., M. Sulis, M. Masbou, S. J. Kollet, and C. Simmer, 2014: A scale-consistent Terrestrial Systems Modeling Platform based on COSMO, CLM, and ParFlow. *Mon. Wea. Rev.,* **142,** 3466–3483, doi:10.1175/MWR-D-14-00029.1.

Simmer, C., and Coauthors, 2015: Monitoring and modeling the terrestrial system from pores to catchments: The Transregional Collaborative Research Center on Patterns in the Soil–Vegetation–Atmosphere System. *Bull. Amer. Meteor. Soc.,* doi:10.1175/BAMS-D-13-00134.1, in press.

Stöckli, R., and Coauthors, 2008: Use of FLUXNET in the Community Land Model development. *J. Geophys. Res.,* **113,** G01025, doi:10.1029/2007JG000562.

Suyker, A. E., and S. B. Verma, 2009: Evapotranspiration of irrigated and rainfed maize–soybean cropping systems. *Agric. For. Meteor.,* **149,** 443–452, doi:10.1016/j.agrformet.2008.09.010.

Taylor, K. E., 2001: Summarizing multiple aspects of model performance in a single diagram. *J. Geophys. Res.,* **106,** 7183–7192, doi:10.1029/2000JD900719.

Thornton, P. E., and N. E. Zimmermann, 2007: An improved canopy integration scheme for a land surface model with prognostic canopy structure. *J. Climate,* **20,** 3902–3923, doi:10.1175/JCLI4222.1.

Tsvetsinskaya, E. A., L. O. Mearns, and W. E. Easterling, 2001: Investigating the effect of seasonal plant growth and development in three-dimensional atmospheric simulations. Part II: Atmospheric response to crop growth and development. *J. Climate,* **14,** 711–729, doi:10.1175/1520-0442(2001)014<0711:ITEOSP>2.0.CO;2.

Valcke, S., 2013: The OASIS3 coupler: A European climate modelling community software. *Geosci. Model Dev.,* **6,** 373–388, doi:10.5194/gmd-6-373-2013.

Van den Hoof, C., E. Hanert, and P. L. Vidale, 2011: Simulating dynamic crop growth with an adapted land surface model—JULES–SUCROS: Model development and validation. *Agric. For. Meteor.,* **151,** 137–153, doi:10.1016/j.agrformet.2010.09.011.

Van Wittenberghe, S., and Coauthors, 2013: Upward and downward solar-induced chlorophyll fluorescence yield indices of four tree species as indicators of traffic pollution in Valencia. *Environ. Pollut.,* **173,** 29–37, doi:10.1016/j.envpol.2012.10.003.

von Caemmerer, S., 2000: *Biochemical Models of Leaf Photosynthesis*. CSIRO Publishing, 165 pp.

Wesseling, J. G., J. A. Elbers, P. Kabat, and B. J. V. den Broek, 1991: SWATRE: Instructions for input. Winand Staring Centre Internal Note, Wageningen, Netherlands.

White, J. W., 2009: Bringing genetics and genomics to crop simulations: Experiences with wheat, sorghum and common bean in solving the GEM-to-P problem. *Crop Modeling and Decision Support,* W. Cao, E. Wang, and J. W. White, Eds., Springer, 44–53.

White, M. A., P. E. Thornton, S. W. Running, and R. R. Nemani, 2000: Parameterization and sensitivity analysis of the BIOME–BGC terrestrial ecosystem model: Net primary production controls. *Earth Interact.,* **4,** doi:10.1175/1087-3562(2000)004<0003:PASAOT>2.0.CO;2.

Wilson, K., and Coauthors, 2002: Energy balance closure at FLUXNET sites. *Agric. For. Meteor.,* **113,** 223–243, doi:10.1016/S0168-1923(02)00109-0.

Wöhling, T., and Coauthors, 2013: Multiresponse, multiobjective calibration as a diagnostic tool to compare accuracy and structural limitations of five coupled soil–plant models and CLM3.5. *Water Resour. Res.,* **49,** 8200–8221, doi:10.1002/2013WR014536.

Wullschleger, S. D., 1993: Biochemical limitations to carbon assimilation in C_3 plants—A retrospective analysis of the A/C_i curves from 109 species. *J. Exp. Bot.,* **44,** 907–920, doi:10.1093/jxb/44.5.907.

Zeng, X., M. Shaikh, Y. Dai, R. E. Dickinson, and R. Myneni, 2002: Coupling of the Common Land Model to the NCAR Community Climate Model. *J. Climate,* **15,** 1832–1854, doi:10.1175/1520-0442(2002)015<1832:COTCLM>2.0.CO;2.